Proceedings of the 21st ICSMGE, Vienna, Austria, 14 – 19 June 2026. Pistrol, Adam & Schweiger (eds.)
Published by: ÖGG, Austrian Society for Geomechanics, Salzburg, Austria, ISBN 978-3-9503898-4-5
https://doi.org/10.53243/ICSMGE2026-319

Interpretation of the cyclic behaviour of a gassy-silty soil by energetic model based on cyclic tests

Kadir Kocaman, Aşkın Özocak
Department of Civil Engineering, Sakarya University, Sakarya, Turkey, kadirkocaman@sakarya.edu.tr

Lucia Mele, Alessandro Flora
Department of Civil, Architectural and Environmental Engineering, University of Naples Federico II, Naples, Italy

ABSTRACT: The presence of air in unsaturated and gassy soils located above groundwater level influence the response of the soils under cyclic loads. The air volume in the pores of soils causes a slow build-up of excessive pore water pressure during cyclic loading compared to saturated soils. Although the studies carried out have made considerable progress in expressing the cyclic behaviour of unsaturated and gassy sands, the effect of the degree of saturation on the cyclic behaviour of silty soils is still a poorly investigated research topic. This study focuses on the experimental investigation of the effect of high saturation degrees (S_r>80%) on the cyclic behaviour of silty soils and its interpretation by energetic model. In the experimental study, medium dense non-plastic silty soil obtained from Sakarya basin, where liquefaction was observed in 1999 Kocaeli earthquake, was used. The behaviour of the specimens reconstituted at in situ density by the moist tamping method was investigated by undrained cyclic triaxial tests. The specimens were saturated to different degrees of saturation by correlating it with B value and loaded at different cyclic stress ratios. It was determined that the decrease in the degree of saturation significantly increases the cyclic resistance. The cyclic resistance at 80% degree of saturation is approximately 1.5 times that of the saturated condition. It was also observed that the energy-based method, which has been successfully practiced in sands, can also be applied to soils contain fines with a great convergence. Thus, it was determined that cyclic resistances at different saturation degrees can be simulated with the energetic model.

KEYWORDS: Gassy silty soil, cyclic resistance, B-value, energetic model.

1 INTRODUCTION

Liquefaction is a phenomenon marked by a rapid loss of soil strength, which can occur in loose, saturated sands subjected to earthquake shaking or other forms of rapid loading. During liquefaction, when the effective stresses approach zero due to an excess pore pressure build-up, soil behaviour switches from that of a solid to that of a fluid. The consequences may be catastrophic, causing serious damage to engineering structures.

However, experimental studies showed that the presence of air into pores of soil can increase liquefaction resistance. Therefore, Induced Partial Saturation (IPS) is used as a mitigation technique against liquefaction (Flora et al., 2021). IPS consists of injecting air in forms of occluded bubbles into pores of soils, reaching high degrees of saturation (say S_r>80%). Non-saturated soils with S_r higher than 80% herein after will be referred to as *gassy soils*.

Experimental studies showed that even a small decrease of the degree of saturation (from 100 to 98%) can increase the resistance to liquefaction by 30% (Yegian et al., 2007, Wang et al., 2016, Mele et al., 2022). Rocker (1968) conducted one of the earliest studies in literature examining the effect of the degree of saturation on clean sands through cyclic tests, using the pore pressure coefficient (B-value) as an indicator. Okamura and Noguchi (2009) stated that reducing the degree of saturation from 100% to 70% increased the liquefaction resistance of sand by a factor of 2,5. Tsukamoto et al. (2014), on the other hand, asserted that liquefaction is not possible in sands with degrees of saturation below 70%.

In recent studies, predicting the behavior of gassy cohesionless soils under cyclic loading has gained increasing attention. Mele and Flora (2019) and Mele et al. (2022) simulated the behavior of gassy sands using an energetic-based model. Seyedi-Viand and Bayat (2021) modeled the liquefaction behavior of partially saturated sands by incorporating the compressibility of the air–water mixture present in the soil pores. Mele et al. (2024a) calibrated the elastoplastic constitutive model proposed by Dafalias and Manzari (2004) using experimental results from two different sandy soils subjected to cyclic loading under gassy conditions and developed model-based predictions for their liquefaction resistance.

However, experimental and numerical researches on the cyclic behavior of gassy soils, have predominantly focused on sands (Rocker, 1968; Yoshimi et al., 1989; Okur and Umu, 2013; Bayat and Gülen, 2020), while the effect of the degree of saturation on the cyclic behaviour of silty soils is still a poorly investigated research topic Recent earthquakes have shown that also silty soils can liquefy. Indeed, during the 1999 Kocaeli earthquake, alluvial silts in the city of Sakarya (Adapazarı) exhibited cyclic failure, resulting in deformations reaching up to 80 cm (Bray et al., 2004; Bol et al., 2010). Furthermore, during the 2011 Christchurch earthquake, widespread liquefaction was observed in areas dominated by non-plastic or low-plasticity silty soils (Cubrinovski et al., 2012; Maurer et al., 2015). These events have intensified research on the cyclic behavior of saturated silty soils but, little has been done on the cyclic behaviour of gassy silty soils. Recently, Banerjee (2017) observed that reducing the degree of saturation from 100% to 97% increased the liquefaction resistance of silts by 25%.

In this study, the behavior of gassy silty sand under cyclic loading was observed, and its compatibility with the energetic approach—previously applied successfully to clean sands—was examined. The experimental program comprised triaxial cyclic tests conducted on low-plasticity silty sand specimens equilibrated at three different B-values. The liquefaction resistance curves obtained from the experiments were interpreted using the energetic approach proposed by Mele and Flora (2019).

2 EXPERIMENTAL STUDY

2.1 *Material*

In this study, the silty soil, coming from Sakarya region (north-western Turkey) was used. The physical properties of Sakarya silty soil are presented in Table 1 (Mele et al., 2024b). According to ASTM D2487, it is classified as low-plasticity silt (ML). Relevant ASTM standards were followed in the physical tests. The grain-size distribution of silt was also given (Figure 1).

Table 1. Physical properties of Sakarya silty soil.

Physical property	Value	Standard
Gs	2,74	ASTM D854
D_{50} (mm)	0,07	ASTM D2487
Cu (D_{60}/D_{10})	14,4	ASTM D2487
Silt (d<0,075 mm) (%)	46,0	ASTM D2487
Clay (d<0,002 mm) (%)	6,3	ASTM D2487
w_p (%)	20,9	ASTM D4318
w_L (%)	27,5	ASTM D4318
Ip (%)	6,6	ASTM D4318
k (m/s)	$1{,}86.\ 10^{-6}$	ASTM D5084
Organic content (%)	9,3	ASTM D2974
e_{max}	1,20	ASTM D4254-06
e_{min}	0,69	ASTM D4253-06
Symbol	ML	ASTM D2487

G_s:Specific gravity, D_{50}:Average soil particle size, C_u:Coefficient of uniformity, e_{max}:Maximum void ratio, e_{min}:Minimum void ratio, w_p:Plastic limit, w_L:Liquid limit, I_p:Plasticity index, k:Coefficient of permeability.

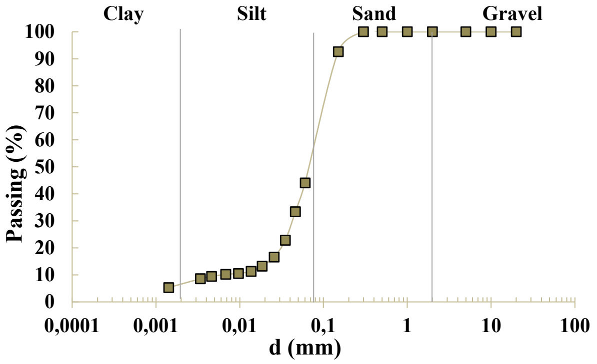

Figure 1. Grain-size distribution curve of silty soil.

2.2 *Specimen preparation*

The specimens used in the triaxial tests were prepared using the moist tamping method. The initial diameter and height of the specimens were 38 mm and 76 mm, respectively. To prepare a semi-saturated specimen (S_r = 50%) with a void ratio (e) of 1.01 (D_r=40%) at the target dimensions, the required amount of dry soil was mixed with water to achieve a water content (w) of 18.1%, forming a soil–water mixture. This mixture was then compacted in five layers within a 38 mm diameter plexiglass split mold to achieve a total height of 76 mm.

2.3 *Cyclic triaxial apparatus and testing procedure*

The conventional Bishop and Wesley (1975) Triaxial Cell was used in this research. The testing system consists of three main components: the triaxial cell, the volume change device, and the pressure control panel (Figure 2). Air pressure is used to generate the water pressure required for applying confining and back pressure. For cyclic loading, a loading piston controlled by water pressure is utilized. Volume change is measured using a calibrated linear transducer (LVDT).

Prior to testing, all components of the triaxial system were saturated using deionized water to ensure full saturation of the apparatus. The triaxial specimens were placed into the cell and subsequently subjected to three consecutive stages: saturation, isotropic consolidation, and undrained cyclic loading. During the saturation stage, the confining pressure (σ_c) and back pressure were simultaneously increased at a constant rate while maintaining a pressure differential of 10 kPa between them (ramping method). In the consolidation stage, the back pressure was kept constant while the confining pressure was raised to achieve isotropic consolidation under the target effective stress (σ' = 50 kPa). In the cyclic loading stage, the consolidated specimens were loaded under undrained conditions at different cyclic stress ratios (CSR) corresponding to three different target B-values. The frequency of cyclic loading (f) was 0.008 Hz.

Figure 2. The cyclic Bishop and Wesley triaxial cell of geotechnical laboratory of University of Naples Federico II (Italy).

3 TEST RESULTS

Table 2 presents the characteristics of the triaxial cyclic tests. A total of eight cyclic triaxial tests were conducted. For saturated specimens, a B-value greater than 0.95 was ensured. For gassy soils, two different B-values (0.50 and 0.20) were employed. The degree of saturation (S_r) of the specimens was estimated using the B value–S_r relationship proposed by Yang (2002) (Figure 3). In testing program S_r is higher than 78% in order to assume that matric suction is negligible. Cyclic failure was evaluated based on two criteria: 5% double-amplitude axial strain ($\varepsilon_{DA5\%}$) and a maximum excess pore water pressure ratio of r_u = 0,9.

Table 2. Testing program of performed cyclic triaxial test.

Test	e	B	S_r%	σ' (kPa)	CSR	$N_{DA,5\%}$	$N_{ru,0.9}$
CTX_100_015	0,99	0,95	100	50	0,15	23,7	22,0
CTX_100_018	0,98	0,98	100	50	0,18	5,7	6,0
CTX_100_019	0,98	0,99	100	50	0,19	3,8	3,6
CTX_100_016	0,99	0,96	100	50	0,16	10,3	10,1
CTX_95_017	0,96	0,50	95	50	0,17	36,2	34,0
CTX_95_020	0,97	0,50	95	50	0,20	6,3	5,1
CTX_78_021	0,99	0,20	78	50	0,21	39,8	39,1
CTX_80_027	0,98	0,21	80	50	0,27	2,9	3,2

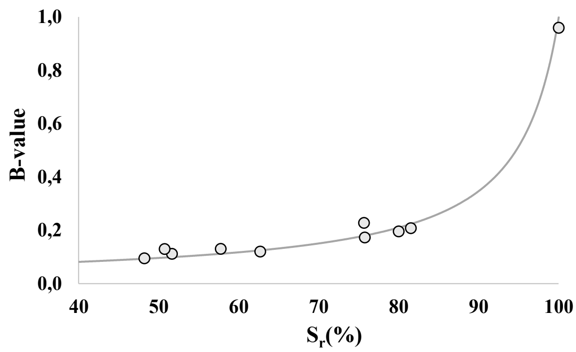

Figure 3. B value-S_r relationship of Sakarya silty soil at D_r=40%.

Figure 4 presents the stress–strain relationships and stress paths of two specimens with different degrees of saturation but similar CSR (0,20 and 0,21). It is evident that variations in the degree of saturation significantly influence cyclic behavior. The increase in the degree of saturation has reduced deformation due to cyclic loading. In specimen CTX_78_021, the coexistence of air and water in the pores prevented a sudden rise in pore water pressure, thereby delaying the loss of effective stress and enabling the soil to maintain its stiffness for a longer period. In contrast, specimen CTX_95_020 exhibited more abrupt cyclic failure.

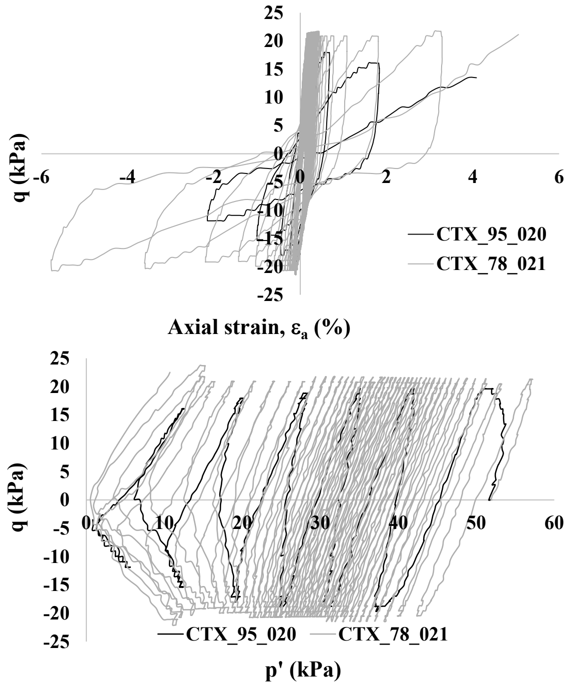

Figure 4. Stress-strain relationship and stress paths of gassy specimens.

Figure 5 illustrates the pore water pressure and axial strain responses for the same specimens. The silty specimen with S_r = 95%, being closer to full saturation, exhibited a rapid increase in pore water pressure under the applied CSR. In contrast, the S_r = 80% specimen, which contained a larger volume of air in the pores, demonstrated a delayed buildup of pore water pressure, as also reported by Fredlund et al. (2012) and Wang et al. (2016). Once the excess pore pressure ratio (r_u) reached approximately 0.40, structural resistance began to degrade rapidly, and the pore pressure increase accelerated. The specimen with S_r = 80% experienced failure after more than 30 additional loading cycles compared to the S_r = 95% specimen.

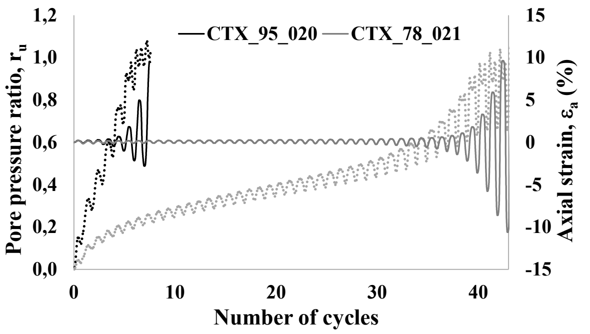

Figure 5. Pore water pressure and axial deformation responses under undrained cyclic loading (S_r=78% and S_r=95%) of two tests performed with a similar CSR.

Figure 6 presents the liquefaction resistance curves of specimens with degrees of saturation S_r = 100%, 95%, and 80% in the CSR–N plane. For defining the liquefaction resistance point, the CSR value corresponding to 15 loading cycles was considered. When the degree of saturation decreased from 100% to 95%, liquefaction resistance increased by approximately 20%. This increase rose to 50% when the saturation decreased to 80%. In other words, a 20% reduction in the degree of saturation resulted in a 1.5-fold increase in liquefaction resistance. With a decrease in the degree of saturation, the air phase in the pores becomes more pronounced, requiring a greater accumulation of cyclic deformation for the increase in r_u corresponding to liquefaction. Accordingly, the soil exhibits higher cyclic resistance (Banerjee, 2017).

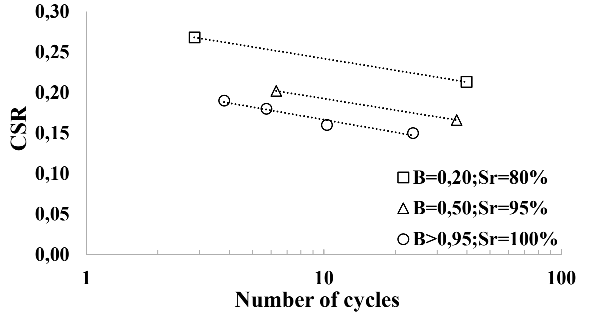

Figure 6. Liquefaction resistance curves for different saturation conditions.

4 ENERGETIC MODEL TO PREDICT LIQUEFACTION RESISTANCE OF GASSY SOILS

To predict liquefaction resistance of gassy soils Mele & Flora (2019) proposed an energetic approach, which is based on the concept of specific volumetric energy to liquefaction ($E_{v,liq}$). It is a synthetic and sound state parameter representing the work spent to reduce soil volume, and can be seen as the sum of three components:

$$E_{v,liq} = E_{v,sk,liq} + E_{w,liq} + E_{air,liq} \tag{1}$$

$E_{v,sk,liq}$, $E_{w,liq}$ and $E_{air,liq}$ represent the specific work done respectively to cause the deformation of the soil skeleton, the flow of water and the flow of air into the pores network. They can be expressed as:

$$E_{v,sk,liq} = \int_0^{\varepsilon_{v,(Nliq)}} [(\sigma - u_a) + sS_{r0}] \cdot d\varepsilon_v \tag{2}$$

$$E_{w,liq} = -\int_{Sr0}^{Sr,liq} \frac{e(S_r)}{1+e(S_r)} s(S_r) \cdot dS_r \tag{3}$$

$$E_{air,liq} = \frac{e_0}{1+e_0}\left(1 - S_{r,0}\right) u_{a,liq} \left(\ln \frac{V_{air,0}}{V_{air,liq}}\right) \tag{4}$$

$E_{v,sk,liq}$ depends on the stress state (σ'_{ns}, where the pedex indicates non saturated condition), on the initial void ratio e_0 and on the initial degree of saturation (S_{r0}), while it depends neither on CSR nor on N_{liq}. Obviously, $E_{v,sk,liq}$=0 for undrained tests on saturated soils. In eq. (2) $d\varepsilon_v$ is the increment of volumetric strain during undrained cyclic loading. Eq. (2) represents the area of the average curve σ'_{ns}-ε_v for a specific soil state. The corresponding extreme of integration $\varepsilon_{v,(Nliq)}$ is the volumetric strain at which liquefaction occurs. For gassy soils, it can be assumed equal to the potential volumetric strain (ε_v*) proposed by Okamura & Soga (2006):

$$\varepsilon_v * = \frac{e_0}{1+e_0} \cdot (1 - S_{r0}) \cdot \left(1 - \frac{u_{a,0}}{\sigma}\right) \tag{5}$$

where e_0, S_{r0} and $u_{a,0}$ are the initial void ratio, degree of saturation and pore air pressure, respectively, while σ is the total stress. The energy of deformation of water (Eq. 3) is due to the change of water content, and depends on matric suction (s). This is generally neglected in gassy soils. Finally, the energy of deformation of air (Eq. 5) describes the effect of pressure variation in the gas phase, where $V_{air;0}$ is the volume of air at the beginning of the shearing phase, and $V_{air;liq}$ is the volume of air corresponding to liquefaction.

According to Mele et al. (2022), known $E_{v,liq}$, CRR of gassy soils (CRR_{ns}) can be estimated from that of saturated one (CRR_s), from the following equation:

$$\Delta CRR_{Nliq} = -105.7 \cdot \left(\frac{E_{v,liq}}{p_a}\right)^2 + 10.2 \cdot \frac{E_{v,liq}}{p_a} \quad (6)$$

where $\Delta CRR = CRR_{ns} - CRR_s$ is computed at a given number of equivalent cycles.

Further details regarding the energetic approach may be found in Mele & Flora (2019) and Mele et al. (2022). Based on the approach of Mele et al., (2022), $E_{v,liq}$ has been calculated for gassy soils of Table 2. Figure 7 shows the simulated liquefaction resistance curves of gassy soils compared with the experimental data. The energy approach validated on sands seems to work satisfactorily also in silty soil coming from Sakarya, even though the liquefaction resistance is a bit overestimated for Sr= 80%. It could be due to the fact that when the degree of saturation is equal or below 80% some meniscus of air-water can be formed and then suction, and then $E_{w,liq}$, cannot be neglected. Further tests will be performed in order to clarify this aspect.

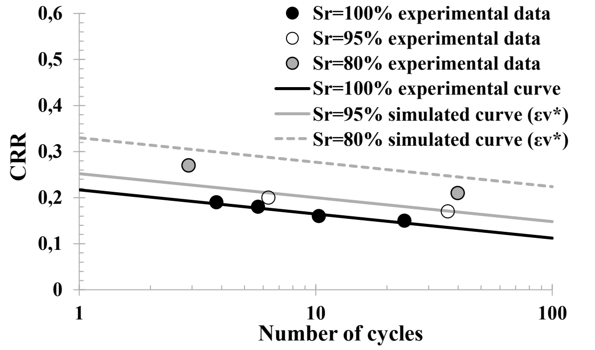

Figure 7. Simulation of liquefaction resistance curves of gassy soils by using energy approach of Mele & Flora (2019).

5 CONCLUSIONS

This study focuses on investigating the cyclic behavior of a silty soil under gassy conditions and interpreting its liquefaction resistance using an energetic model. The testing program includes cyclic triaxial tests conducted on a natural low-plasticity silty soil from Sakarya, prepared at three different degrees of saturation. The test results were interpreted using the energetic approach developed by Mele & Flora (2019), and model curves were constructed to estimate liquefaction resistance. As the degree of saturation decreased, the development of excess pore water pressure was delayed. The prolonged presence of effective stress limited deformations within a low number of loading cycles. In the case of $S_r = 80\%$, the liquefaction resistance was 1.5 times higher than that of the fully saturated condition. It was observed that the energetic approach proposed by Mele & Flora (2019), which has yielded satisfactory results for sands, can also be applied to silty soils.

6 ACKNOWLEDGEMENTS

This study was supported by TUBITAK (Scientific and Technological Research Council of Turkey) under Programme 2214-A (International Research Fellowship Programme for PhD Students).

7 REFERENCES

Banerjee, A. 2017. *Response of unsaturated soils under monotonic and dynamic loading over moderate suction states* (doctoral dissertation). University of Texas Arlington.

Bayat, E. E., and Gulen, D. B. 2020. Undrained dynamic response of partially saturated sands tested in a DSS-C device. *Journal of Geotechnical and Geoenvironmental Engineering* 146(11), 04020118.

Bishop, A. W., and Wesley, L. D. 1975. A hydraulic triaxial apparatus for controlled stress path testing. *Geotechnique* 25(4), 657-670.

Bol, E., Önalp, A., Arel, E., Sert, S., and Özocak, A. 2010. Liquefaction of silts: the Adapazari criteria. *Bulletin of Earthquake Engineering* 8, 859-873.

Bray, J. D., Sancio, R. B., Durgunoglu, T., Onalp, A., Youd, T. L., Stewart, J. P., ... and Karadayilar, T. 2004. Subsurface characterization at ground failure sites in Adapazari, Turkey. *Journal of Geotechnical and Geoenvironmental Engineering* 130(7), 673-685.

Cubrinovski, M., Robinson, K., Taylor, M., Hughes, M., and Orense, R. 2012. Lateral spreading and its impacts in urban areas in the 2010–2011 Christchurch earthquakes. *New Zealand Journal of Geology and Geophysics* 55(3), 255-269.

Dafalias, Y. F., and Manzari, M. T. 2004. Simple plasticity sand model accounting for fabric change effects. *Journal of Engineering Mechanics* 130(6), 622-634.

Flora, A., Bilotta, E., Chiaradonna, A., Lirer, S., Mele, L., and Pingue, L. (2021). A field trial to test the efficiency of induced partial saturation and horizontal drains to mitigate the susceptibility of soils to liquefaction. *Bulletin of Earthquake Engineering*, *19*, 3835-3864.

Fredlund, D. G., Rahardjo, H., and Fredlund, M. D. (2012). Soil mechanics for unsaturated soils. John Wiley & Sons.

Maurer, B. W., Green, R. A., Cubrinovski, M., and Bradley, B. A. 2015. Fines-content effects on liquefaction hazard evaluation for infrastructure in Christchurch, *New Zealand. Soil Dynamics and Earthquake Engineering* 76, 58-68.

Mele, L., and Flora, A. 2019. On the prediction of liquefaction resistance of unsaturated sands. *Soil Dynamics and Earthquake Engineering* 125, 105689.

Mele, L., Kocaman, K., Özocak, A., and Flora, A. 2024b. Instability Conditions of a Silty Sand under Monotonic Loads in Simple Shear Tests. *Journal of Geotechnical and Geoenvironmental Engineering* 150(11), 04024116.

Mele, L., Lirer, S., and Flora, A. 2022. An energetic interpretation of liquefaction laboratory tests on partially saturated soils. *Journal of Geotechnical and Geoenvironmental Engineering* 148(10), 04022082.

Mele, L., Marinelli, F., Lirer, S., and Flora, A. 2024a. Model prediction of cyclic liquefaction resistance of gassy soils. *Acta Geotechnica* 19(7), 4415-4435.

Okamura, M., and Noguchi, K. 2009. Liquefaction resistances of unsaturated non-plastic silt. *Soils and Foundations* 49(2), 221-229.

Okamura, M., & Soga, Y. 2006. Effects of pore fluid compressibility on liquefaction resistance of partially saturated sand. Soils and Foundations, 46(5), 695-700.

Okur, V., and Umu, S. U. 2013. Energy approach to unsaturated cyclic strength of sand. *Bulletin of Earthquake Engineering* 11, 503-519.

Rocker, K. 1968. *The liquefaction behavior of sands subjected to cyclic loading*. Doctoral dissertation, Massachusetts Institute of Technology.

Seyedi-Viand, S. M., and Eseller-Bayat, E. E. 2021. An alternative empirical function to predict air–water mixture bulk modulus for numerical modeling of liquefaction behavior of induced partially saturated sands. *Bulletin of Earthquake Engineering* 19(5), 1987-2011.

Tsukamoto, Y., Kawabe, S., Matsumoto, J., and Hagiwara, S. 2014. Cyclic resistance of two unsaturated silty sands against soil liquefaction. *Soils and Foundations* 54(6), 1094-1103.

Wang, H., Koseki, J., Sato, T., Chiaro, G., and Tian, J. T. 2016. Effect of saturation on liquefaction resistance of iron ore fines and two sandy soils. *Soils and Foundations* 56(4), 732-744.

Yang, J. 2002. Liquefaction resistance of sand in relation to P-wave velocity. *Geotechnique* 52(4), 295-298.

Yegian, M. K., Eseller-Bayat, E., Alshawabkeh, A. & Ali, S. (2007). Induced-partial saturation for liquefaction mitigation: exper imental investigation. J. Geotech. Geoenviron. Engng ASCE 133, No. 4, 372–380.

Yoshimi, Y., Tanaka, K., and Tokimatsu, K. 1989. Liquefaction resistance of a partially saturated sand. *Soils and Foundations* 29(3), 157-162.